Advances in Radiation Oncology (2022) 000, 100936

advances in radiation oncology

www.advancesradonc.org

Special Collection

Radiopharmaceuticals as Novel Immune System Tracers

Natalie A. Ridge, DO, MS,[a,*] Anne Rajkumar-Calkins, MD,[b] Stephanie O. Dudzinski, MD, PhD,[b] Austin N. Kirschner, MD, PhD,[b] and Neil B. Newman, MD, MSc[a]

[a]*Department of Radiation Oncology, University of Texas Health Science Center at San Antonio, San Antonio, Texas;*
[b]*Department of Radiation Oncology, Vanderbilt University Medical Center, Nashville, Tennessee*

Received November 3, 2021; accepted February 7, 2022

Abstract

Immune checkpoint inhibitors (ICIs) have transformed the treatment paradigms for multiple cancers. However, ICI therapy often fails to generate measurable and sustained antitumor responses, and clinically meaningful benefits remain limited to a small proportion of overall patients. A major obstacle to development and effective application of novel therapeutic regimens is optimized patient selection and response assessment. Noninvasive imaging using novel immunoconjugate radiopharmaceuticals (immuno−positron emission tomography and immuno-single-photon emission computed tomography) can assess for expression of cell surface immune markers, such as programmed cell death protein ligand-1 (PD-L1), akin to a virtual biopsy. This emerging technology has the potential to provide clinicians with a quantitative, specific, real-time evaluation of immunologic responses relative to cancer burden in the body. We discuss the rationale for using noninvasive molecular imaging of the programmed cell death protein-1 and PD-L1 axis as a biomarker for immunotherapy and summarize the current status of preclinical and clinical studies examining PD-L1 immuno −positron emission tomography. The strategies described in this review provide insight for future clinical trials exploring the use of immune checkpoint imaging as a biomarker for both ICI and radiation therapy, and for the rational design of combinatorial therapeutic regimens.

Introduction

Immune checkpoint inhibitors (ICIs) have markedly improved clinical outcomes for both localized and metastatic neoplasms. Ipilimumab, a human monoclonal antibody (mAb) targeting immune checkpoint molecule cytotoxic T lymphocyte associated protein 4 (CTLA-4), was the first ICI to receive Food and Drug Administration (FDA) approval (in 2011), based on a landmark trial showing the drug significantly improved overall survival in patients with metastatic melanoma.[1] The clinical success of ipilimumab paved the way for development of mAbs targeting a distinct immune checkpoint pathway: programmed cell death protein-1 (PD-1) and its ligand (PD-L1). Subsequent large-scale trials proved anti-PD-1 and anti-PD-L1 antibodies to be one of the most successful immunotherapeutic strategies to enhance antitumor responses and improve overall survival across a spectrum of malignancies.[2-6] To-date, there have been 6 ICI drugs targeting the PD-1/PD-L1 signaling pathway that have

Sources of support: This work had no specific funding.

Disclosures: The authors declare that they have no known competing financial interests or personal relationships that could have appeared to influence the work reported in this paper.

*Corresponding author.; E-mail: ridgen@uthscsa.edu

https://doi.org/10.1016/j.adro.2022.100936

been FDA-approved, with indications for nineteen cancer types and 2 tissue-agnostic conditions.[7]

Despite undeniable progress of ICIs in cancer treatment, they are not without their limitations. One major obstacle is primary and acquired resistance to ICI therapy. Clinical responses to ICI monotherapy remain limited to a small proportion of patients, and many patients who initially respond ultimately progress through treatment. Anti-PD-1/PD-L1 antibodies have highly heterogenous clinical efficacy, with overall response rates of <5% to >40% across cancer types.[8,9] Another important limitation is the potential for off-target toxicities related to excessive immune activation. Although standard ICI regimens are generally well-tolerated, particularly in comparison to conventional systemic treatments, the risk of associated grade ≥3 treatment-related adverse events can be 10% to 30% depending on the drug, dose, and duration of therapy[10] (Table 1). Lastly, although the benefits that patients can derive from ICI therapy can be clinically significant, these drugs are also associated with substantial financial costs. For PD-1/PD-L1 inhibitor therapy, the annual cost per patient is ≥$150,000, with even higher costs associated with anti-CTLA-4 therapy.[11]

Due to the large proportion of nonresponding malignancies, risk of severe treatment-related complications, and considerable cost of ICI therapies, there is a pressing need to optimize strategies for tailoring personalized treatment regimens, and for real-time assessment of therapeutic responses. Establishment of reliable, specific predictive biomarkers for ICI response will further provide new insights into key modifiers of patient outcomes and will also be central to identifying optimal synergistic strategies. There have been many recent and ongoing studies exploring methods to improve response rates, including combining ICI with conventional treatment modalities such as radiation therapy (RT).[12-15]

Expression of PD-L1 on tumor cells or tumor-infiltrating immune cells correlates with higher response rates to ICI therapy,[16] and clinical treatment decisions are often guided by PD-L1 expression status assessed via standardized immunohistochemistry (IHC) assays using a single pretreatment tumor biopsy sample. However, there are many inherent technical and biological limitations of IHC which, in addition to the dynamic nature of PD-L1 expression and immune responses to tumors, restrict its predictive value and clinical utility. Therefore, there is a need to establish standardized complementary methods to capture and quantify PD-L1 expression in a way that augments the value of tissue-based assays. Noninvasive molecular imaging using novel immunoconjugate radiopharmaceuticals (immuno-PET or immuno-SPECT) could represent an ideal methodology in this respect.

Recent technological advancements in radiopharmaceuticals permit targeted imaging of specific markers on the cell surface. In patients with newly diagnosed or recurrent prostate cancer, prostate specific membrane antigen (PSMA)-based positron-emission tomography (PET) can now identify areas of active disease which were previously undetected.[17] This can aid in patient- and target-identification for metastasis-directed radiation therapy for better outcomes.[18] Radiopharmaceutical probes can also be designed to target various immune markers within the tumor microenvironment (TME), including PD-L1, to select patients most likely to benefit from a particular immunotherapy. Furthermore, whole-body imaging could help to distinguish immunogenic ("hot") tumors from nonimmunogenic ("cold") tumors within a patient. In this way, similar to PSMA-PET, molecular imaging of TME components may enable identification of optimal radiation targets (ie, nonimmunogenic tumors that can be irradiated to create an immunogenic TME) primed to respond to release of the PD-1 immune checkpoint. Evolving imaging techniques using modern radiopharmaceuticals therefore hold promise to improve personalized cancer care by guiding ICI treatment selection and informing optimal therapeutically synergistic regimens.

PD-1/PD-L1 Immune Checkpoint Pathway

PD-1 (CD279) is a cell surface receptor that is inducibly expressed on activated CD4+ and CD8+ T cells, B cells, myeloid cells, and some dendritic and natural killer cell subsets.[19] In CD8+ T cells, PD-1 transcription is rapidly and transiently induced upon stimulation through the T cell receptor, with multiple posttranslational modifications regulating the level and duration of cell-surface expression.[20] Under conditions of chronic antigen-specific signaling, PD-1 expression is sustained at a substantially higher level than observed on functional effector and memory CD8+ T cells, and is associated with T cell exhaustion.[21] PD-1 recognizes 2 cognate ligands, PD-L1 (B7-H1) and PD-L2 (B7-H2), which have overlapping but distinct expression patterns. Under physiological conditions, PD-L1 is constitutively expressed on activated T cells, B cells, dendritics, myeloid cells, and a variety of nonhematopoietic cells, including hepatocytes and vascular endothelial cells, and in various immune privileged organs. PD-L1 expression can also be induced and upregulated in the setting of inflammation.[22]

In simplistic terms, binding of PD-1 on activated antigen-specific T cells to its primary ligand, PD-L1, attenuates T cell receptor signaling, thereby inhibiting downstream effector functions and clonal expansion while promoting T cell apoptosis and anergy.[23] This signaling pathway plays an important role in maintenance of peripheral tolerance and limiting immune-mediated tissue damage during acute infection and inflammation. The role of the PD-1/PD-L1 axis in negative regulation of immune responses is well characterized in oncology: tumors exploit the pathway by overexpressing PD-L1 to subvert T-cell mediated immune clearance. Expression of

Table 1 Reported frequencies of various treatment-related adverse events for immune checkpoint inhibitors

		Any grade (grade ≥3)							
Drug	**Study**	**Diarrhea**	**Colitis**	**Pneumonitis**	**Hepatitis**	**Rashes**	**Neurologic**	**Endocrinopathy**	**Any treatment-related event ≥ grade 3**
Pembrolizumab	KEYNOTE-001 (NSCLC)[26]	8.1% (0.6%)	-	3.6% (1.8%)	-	9.7% (0.2%)	-	6.9% (0.2%)	9.5%
	KEYNOTE-001 (melanoma)[29]	16% (2%)	2.7% (1.9%)	1% (0.1%)	1.4% (1.4%)	14% (0%)	-	15% (1%)	12%
	KEYNOTE-010[27]	7% (0.3%)	1% (0.6%)	5% (2%)	1% (0%)	11% (0.3%)	-	15% (1%)	14%
	KEYNOTE-024 [6]	14.3% (3.9%)	1.9% (1.3%)	5.8% (2.6%)	6% (0.73%)	3.9% (3.9%)*	1.6% (0%)	19% (2%)	26.6%
Nivolumab	CA209-003[124]	14.8% (1.1%)	-	5.2% (1.5%)	7% (1.9%)†	16% (0%)	-	10.7% (0.7%)	17%
	CheckMate 026[33]	14% (1%)	1% (0.75%)	2.6% (1.5%)	16% (5%)†	26% (10%)	1% (1%)‡,§	6.7% (0.4%)	18%
	Weber et al[125]	12.7% (0.5%)	1% (0.7%)	1.7% (0%)	0.2% (0.2%)	12.7% (0.3%)	1% (1%)‖,¶	7.8% (0.3%)	10%
Cemiplimab	Migden et al[126]	27% (0%)	-	4% (1%)	0% (1%)	23% (0%)	0% (1%)‡	10% (0%)	50%
Atezolizumab	OAK[31]	15.4% (0.7%)	0.3% (0%)	1% (0.7%)	0.3% (0.3%)	-	-	-	15%
	IMvigor210[34]	12% (2%)	1% (1%)	-	1% (1%)	5% (1%)	-	8% (0%)	16.8%
Avelumab	JAVELIN Lung[127]	6% (0%)	1% (0.5%)	3% (1%)	1% (1%)	6% (-)	2% (1%)‡,§	9% (1%)	10%
	JAVELIN Solid Tumor[128]	7% (0%)	-	1% (1%)	1.6% (1.1%)†	-	1% (1%)#	7% (0%)	12.5%
Durvalumab	ATLANTIC[129]	0.7% (0.2%)	0.4% (0%)	2% (0.7%)	0.7% (0.7%)†	0.7% (0.2%)	-	10.1% (0.5%)	9%
Ipilimumab	EORTC 18071[130]	41% (98%)	15.5% (8.2%)	-	24.4% (10.9%)†	34% (1.1%)	4.5% (1.9%)	37.8% (7.8%)	55%
	Hodi et al[1]	27% (4.6%)	7.6% (5.3%)	-	3.8% (0%)	19% (0.8%)	-	7.6% (3.8%)	26%
Ipilimumab plus nivolumab	CheckMate 067[131]	45% (9%)	13% (8%)	7% (1%)	33% (20%)	30% (3%)	-	34% (6%)	59.4%

Abbreviation: NSCLC = non−small cell lung cancer.
* Severe skin reactions.
† Transaminase.
‡ Encephalitis.
§ Neuropathy.
‖ Central demyelination.
¶ Guillian-Barré syndrome.
# Monoplegia.

PD-L1 in tumors strongly correlates with advanced disease in multiple cancer types.[24] The premise of anti-PD-1/PD-L1 therapy is to disrupt this inhibitory signaling pathway at the tumor site, restoring effector function of tumor-antigen specific T cells.

Biomarkers of response to PD-1/PD-L1 checkpoint blockade

Consistent with the current knowledge of anti-PD-1/PD-L1 therapy, it is logical to surmise that tumors that overexpress PD-L1 would derive the greatest clinical response. As such, patient selection for anti-PD-1/PD-L1 therapy is most often guided by PD-L1 expression within the pretreatment tumor. PD-L1 testing requirement vary by treatment indication and regimen; 4 of the 6 FDA-approved drugs targeting the PD-1/PD-L1 axis (pembrolizumab, nivolumab, atezolizumab, and cemiplimab) require determination of PD-L1 expression by an FDA-approved companion diagnostic assay, and prespecified thresholds must be met to consider treatment for certain indications. These thresholds vary both within and across tumor types for each drug. The current gold standard method for measuring PD-L1 expression is via IHC staining of tumor samples, which are obtained at the time of diagnosis from invasive biopsy procedures or from surgical specimens. Each commercially available IHC assay varies in method of interpretation, using PD-L1 expression on tumor cells, tumor-infiltrating immune cells, or both, to determine positivity.[25]

The rationale for using PD-L1 as a predictive biomarker initially stemmed from several of the pivotal trials that paved the way for drug approval. A pilot study of anti-PD-1 therapy with nivolumab for a variety of advanced solid tumors showed that 59.5% of patients tested for PD-L1 expression had at least one positive lesion, as defined by a per specimen threshold of ≥5% of tumor cells staining positive by IHC on pretreatment archival samples.[4] Among patients with any PD-L1 positive tumors, an overall response rate (ORR) of 36% was observed, compared with 0% ORR in PD-L1 negative patients. In another seminal phase I study, KEYNOTE-001, a cohort of patients with advanced non−small cell lung cancer (NSCLC) were screened for tumor PD-L1 expression by IHC, with positive status defined as staining in at least 1% of cells (within tumor nests consisting of neoplastic and infiltrating mononuclear cells).[26] Patients who screened positive for PD-L1 expression and received anti-PD-1 therapy with pembrolizumab showed an ORR of 19.4%; however, subgroup analysis revealed an association between response rate and PD-L1 IHC positivity score, and longer progression-free survival (PFS) and OS in patients with ≥50% tumor cell staining positivity, versus patients with an IHC score of <50%. Follow-up studies (KEYNOTE-010[27] and KEYNOTE-024[6]) recapitulated these findings, showing favorable efficacy of PD-1 blockade in high-PD-L1 expressing patients. In a separate KEYNOTE-001 cohort, patients with advanced melanoma were treated with pembrolizumab, after pretreatment IHC evaluation of tumor PD-L1 expression status. Again, PD-L1 expression was found to correlate with clinical outcomes, with higher ORR, PFS, and OS observed among patients with PD-L1 positive tumors (≥1%).[28] Of note, PD-L1 IHC for melanoma used a distinct assay platform and scoring system from those used for NSCLC.

However, these trials and others[29-33] also demonstrate that substantial clinical responses to ICI therapy are possible in patients whose tumors stained negative for PD-L1 by IHC. Additional studies have shown significant antitumor activity regardless of PD-L1 expression, and no association between PD-L1 IHC positivity and enhanced ICI responses.[34,35] We summarize the wide variability in response rates and PD-L1 expression reported in major clinical studies in Table 2. Such discrepancy may be attributed to several technical and biological factors (Fig. 1).

Along with potential variability in IHC assay performance,[36,37] interobserver reproducibility,[38] and age and condition of tissue specimen available for staining,[39] semiquantitative evaluation of tumor PD-L1 expression using tissue-based approaches has several inherent limitations to accurately representing a patient's PD-L1 status. First, staining is generally performed using a single tissue section from a pretreatment biopsy, and in the setting of advanced disease, from a single-tumor or metastatic lymph node specimen. However, solid tumors are heterogenous, with many coexisting subclone populations. These subclones evolve in different areas of the tumor, and vary considerably in their phenotypic and behavioral characteristics, due to unique genetic and epigenetic changes and adaptive responses to microenvironmental pressures. By the same token, PD-L1 expression is a dynamic and nonuniform rather than a static tumor characteristic, and often a high degree of intra- and interlesional expression heterogeneity is observed within a single patient.[40-43] Tumor heterogeneity is also observed between a given primary tumor and its later recurrences and metastatic lesions.[44] Furthermore, PD-L1 expression is observed to fluctuate in response to recent therapies received, including upregulation after RT.[45,46]

A single biopsy sample fails to capture this spatial and temporal heterogeneity, creating often unrecognized sampling error. For example, most studies examining the correlation between efficacy of PD-1/PD-L1 inhibitors and tumor PD-L1 expression do not differentiate the type of material used for testing (biopsy vs resection specimen, often obtained many weeks after initial biopsy or after treatments received). Munari et al showed that discordance between NSCLC core biopsy specimens of a tumor may occur in up to 20% of cases with a 1% cutoff for PD-L1 positive cells,[47] and that 4 or more biopsy specimens are required to accurately classify PD-L1 status by a validated IHC assay.[48] Therefore, relying on PD-L1 IHC as a standalone biomarker to stratify patients for ICI would be

Table 2 Objective response rate varies widely with PD-L1 expression thresholds across clinical studies

Study	Drug	Disease	PD-L1 threshold for positivity	ORR (above/below threshold)
KEYNOTE-001[26]	Pembrolizumab	NSCLC	1%	19%
			50%	45%
		Melanoma	1%	33%
KEYNOTE-010[27]	Pembrolizumab	NSCLC	1%	16%/10%
			50%	45%/NS
KEYNOTE-024[6]	Pembrolizumab	NSCLC	50%	45%/NS
KEYNOTE-006[29]	Pembrolizumab	Melanoma	1%	33%/NS
KEYNOTE-045[132]	Pembrolizumab	Urothelial	10%	22%/21%
CA209-003[133]	Nivolumab	Melanoma	none	32%/NS
		RCC		29%/NS
		NSCLC		17%/NS
		Pooled	5%	36%/0%
OAK[31]	Atezolizumab	NSCLC	1%	18%/8%
			50%	33%/NS
IMvigor210[34]	Atezolizumab	Urothelial	1%	21%/21%
			5%	28%/NS
CheckMate 026[33]	Nivolumab	NSCLC	5%	26%/NS
CheckMate 032[134]	Nivolumab	Urothelial	1%	24%/26%
			5%	28.6%/24.5%

Abbreviations: NSCLC = non−small cell lung cancer; ORR = objective response rate; PD-L1 = programmed death-ligand 1; RCC = renal cell carcinoma.

expected to misclassify and exclude some patients who would benefit from therapy. One way to improve the predictive value of PD-L1 IHC might be to obtain fresh biopsy specimens at the time a treatment regimen is being considered, and to test multiple specimens from a single patient using a tissue microarray. However, given the invasive nature of a biopsy procedure, this would be far less preferred than an alternative noninvasive biomarker. Longitudinal monitoring of expression status during therapy by serial biopsy would be even less practical. Due to all of these factors, novel predictive biomarkers to guide patient stratification and optimize therapeutic benefits of ICIs are urgently needed. Imaging-based methodologies represent an ideal prospect for several reasons, including being noninvasive, easily used for serial evaluation, and providing whole-tumor and whole-patient information.

Conventional Imaging Methods for Predicting and Evaluating Immunotherapy Responses

Different standard imaging modalities are used in the initial pretherapy evaluation of cancer and for monitoring of treatment responses. The most widely used methodologies are contrast-enhanced CT and MRI. Conventional protocols for response measurement by anatomic imaging, including the revised CT Response Evaluation Criteria in Solid Tumors (RECIST v. 1.1), are based on changes in tumor size and do not take into consideration unique response patterns observed with immunotherapies. To this end, modified strategies, such as the immune-related response criteria, immune RECIST, and immune-modified RECIST, have been adopted for assessment of responses in the clinic and implementation in immunotherapy studies.[49-51] These guidelines reclassify disease progression, accounting for possible pseudoprogression due to immune cell infiltration. Although using these newer guidelines may capture patients with pseudoprogression, which might otherwise be misclassified as progressive disease by RECIST 1.1 criteria leading to inappropriate discontinuation of a beneficial treatment, continuation of an ultimately ineffective treatment past radiographic progression also increases risk for poor clinical outcomes.

Radiomics has been studied as one approach to help discriminate between pseudoprogression and true progression (using magnetic resonance imaging), as well as to predict responses before the initiation of

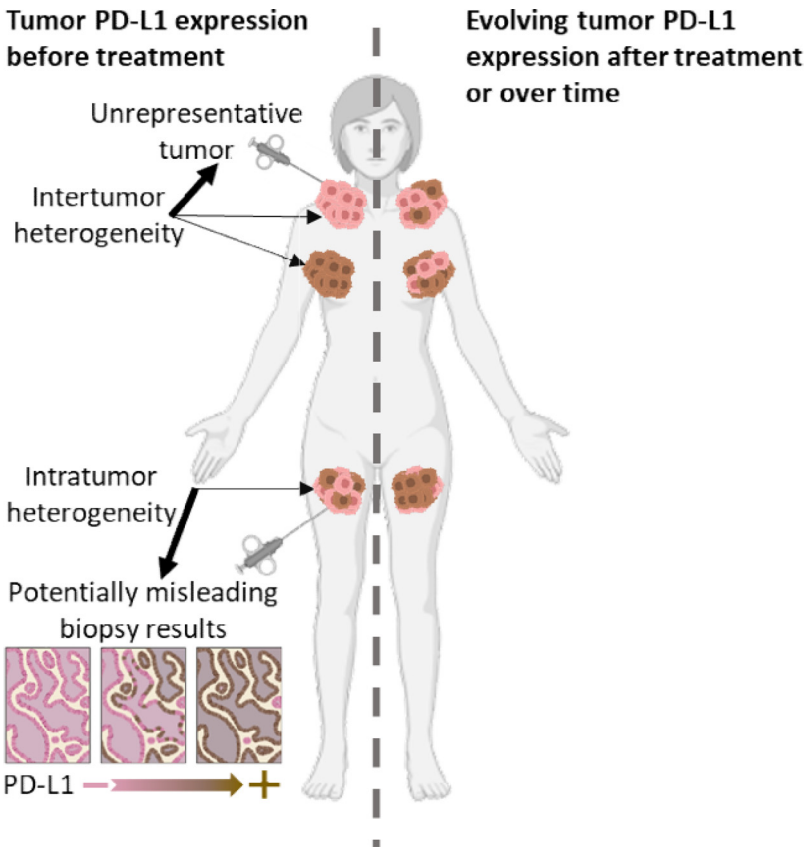

Fig. 1 The disadvantages of PD-L1 (programmed death-ligand 1) quantification via immunohistochemistry. Created with Biorender.com.

immunotherapy. Radiomics models to describe tumor phenotype are created via extraction from standard-of-care images of a large number of quantitative features, based on intensity, size, shape, volume, and texture.[52] One study by Tang et al[53] identified features on pretreatment CT that were associated with tumor PD-L1 expression and T cell density in NSCLC surgical pathology specimens, and established an algorithm that successfully discerned patients with an "immune-activated" phenotype associated with improved overall survival. Another study developed a radiomics model based on pretreatment CT images that predicted hyperprogression in NSCLC patients receiving ICIs.[54] Despite the wide range of possible applications, radiomics models have several inherent limitations, including the time-consuming and subjective process of tumor volume delineation, and lack of universal imaging acquisition protocols across institutions.

PET/CT using [fluorine-18]fluorodeoxyglucose (^{18}F-FDG) tracer is the most common functional tumor imaging technique used in clinical practice, and is routinely used in diagnostic workups, treatment planning, including radiation therapy target delineation, and treatment response evaluation.[55-58] FDG PET has also shown potential as a prognostic and predictive tool in the context of immunotherapy. In a prospective study of a small cohort of advanced NSCLC patients, Kaira et al[59] showed that decrease in FDG lesion uptake between baseline and 1 month better predicted early response to nivolumab therapy than standard CT. In a larger cohort of NSCLC patients, Chardin et al[60] demonstrated a correlation between high baseline metabolic tumor volume, early treatment discontinuation, and poor overall survival after ICI therapy. However, in contrast, other studies have found low tumor FDG uptake to predict poor outcomes after initiation of immunotherapy.[61,62] These conflicting findings highlight that using FDG PET to predict immunotherapy response is not straightforward. An important limitation of this modality is its inability to discriminate if tracer uptake, which is a surrogate for cellular metabolism, is occurring in tumor, stroma, or immune cells. Furthermore, other processes such as necrosis and nonspecific inflammation can influence local FDG uptake, adding to the challenge of interpretation. Accordingly, novel PET tracers that target specific cells or receptors have been developed to evaluate the tumor immune milieu.

Noninvasive molecular imaging of the PD-1/PD-L1 axis

An ideal complementary diagnostic for PD-1/PD-L1 inhibitor therapy should be noninvasive, have the potential for wide availability, and supplement conventional diagnostic tests and biomarkers. Molecular imaging fits these criteria and is one way to overcome many of the weaknesses of tissue-based assays. With broad adoption, it may elucidate the complex interplay between the immune system and tumors as they coevolve during various therapeutic regimens, which is central to understanding cancer in a clinically significant context.

Immuno-PET (positron emission tomography) and immuno-SPECT (single-photon emission computed tomography) have been developed as techniques to noninvasively monitor molecular biomarkers, including PD-L1, across the whole body in real-time. Immuno-PET/SPECT also enable visualization of the spatial distribution of protein expression within and between tumors, and serial imaging provides longitudinal information about therapeutic targets in response to treatment.

Various tracers composed of a chelated radiometal, bound to an antibody or other targeting scaffold with PD-L1 molecular specificity, have shown promise in preclinical models. Several first-in-human studies have been completed, and many more are ongoing.

Preclinical progress in PD-L1 imaging

The potential of PD-L1 imaging was first demonstrated in preclinical models that used whole antibodies conjugated to various radionuclides to visualize PD-L1 expression in tumor-bearing mice.[63-74] These models established initial proof-of-concept, showing that radiolabeled anti-PD-L1 mAb can identify syngeneic and human xenograft tumors expressing PD-L1, and that it can serve as an in vivo biomarker of response to anti-PD-L1 therapy.

Several important principles were learned from these studies that are relevant to translating PD-L1 imaging into clinical trials and practice. For one, it was discovered that added carrier (unlabeled antibody) is necessary in most antibody-based tracer formulations to block sequestration of the radiolabeled antibody in PD-L1 rich nontumor normal tissues (eg, liver, spleen, kidneys, lymph nodes, and bowel) due to low-affinity and nonspecific antibody binding, to allow sufficient tracer to remain in circulation for slower tumor uptake and for optimal tumor-to-background ratios.[68-70,75] Additionally, optimal imaging delay is dependent on probe size, in addition to radioisotope. For intact antibodies, image acquisition at >48 hours, 6 days postinfusion is advantageous as it provides sufficient time for clearance from circulation, which is a relatively slow process (half-lives of days to weeks) for these relatively large proteins.[76] This is in contrast to many standard PET protocols, which use imaging times of 50 to 70 minutes postinjection for rapidly metabolized small molecule tracers such as FDG. Accordingly, the use of longer-lived radionuclides (eg, ^{89}Zr, $t_{1/2}$ = 78.4 hr) for antibody labeling is preferable to shorter-lived ones (eg, ^{18}F, $t_{1/2}$ = 110 min, or ^{64}Cu, $t_{1/2}$ = 12.7 hr), because their half-lives approach the biological half-life of the antibody protein.[69,70,72,77] Thus optimal imaging delay for ^{89}Zr-labeled whole antibody, for instance, is 5 to 7 days postinjection, whereas for a much smaller probe labeled with a shorter-lived radionuclides, such as ^{18}F-BMS-986192 (small protein "adnectin"), images can be acquired within 1 hour. The advantages and limitations of various immunoPET tracers and radionuclides are summarized in Tables 3 and 4.

Perhaps most relevant to clinical translation, and an early indicator of promising utility of PD-L1 imaging in clinical radiation oncology, several preclinical studies demonstrated that immunoPET can be used to monitor RT-induced changes in PD-L1 expression in real-time.[64,73,74] Kikuchi et al[64] used a ^{89}Zr-labeled murine anti-PD-L1 mAb to evaluate PD-L1 expression pre- and postfractionated RT in syngeneic mouse models of HPV and head and neck squamous cell carcinoma and melanoma. They observed RT-induced PD-L1 upregulation in melanoma tumors after 8 Gy in 4 fractions, and in head and neck squamous cell carcinoma tumors after 20 Gy in 10 fractions, using immuno-PET, with confirmation by flow cytometry. In a similar study, Ehlerding et al[73] used cross-reactive ^{89}Zr-atezolizumab to monitor RT-induced changes in mouse xenografts of a human lung cancer cell line with endogenous PD-L1 expression. They showed low tracer uptake at baseline in nonirradiated tumors and increased uptake in response to 2 different radiation regimens (5 Gy in 1 fraction, and 10 Gy in 5 fractions). As a control, they imaged mice bearing PD-L1-negative tumors (A549) and found no appreciable increase in uptake post-RT. Christensen et al[74] also used a cross-reactive ^{89}Zr-labeled mAb to evaluate therapy-induced changes in a syngeneic mouse colon carcinoma model. In this study, tumor-bearing mice were treated with either fractionated RT (6 Gy in 3 fractions) or anti-PD-L1 antibody alone, or with a combination regimen of RT and sequential anti-PD-L1 antibody. PET images were obtained after RT, before the start of anti-PD-L1 therapy. Tumor-localized RT increased PD-L1 tracer uptake both in tumors and spleen, suggesting that RT induces PD-L1 upregulation in circulating immune cells, as well as within tumors. Most notably, maximum tumor tracer uptake correlated with response to anti-PD-L1 therapy (alone and combined with RT), implying that ^{89}Zr-anti-PD-L1 PET has value as a predictive biomarker not only for ICI monotherapy, but also independently for combined-therapy regimens. Together, these data provide insight for the

Table 3 Characteristics of key radionuclides used in immunoPET

Radionuclide	$T_{1/2}$	Advantages	Limitations
^{124}I	100.2 h	$T_{1/2}$ matches circulating $t_{1/2}$ of mAbs Nonresidualizing, low background signal in non-target tissues widely available	Higher radiation exposure to normal organs than shorter-lived isotopes Nonresidualizing, loss of signal in target tissues over time Long positron range (lower spatial resolution) High cost of production
^{89}Zr	78.4 h	Most well-studied for use with immunoPET $T_{1/2}$ matches circulating $t_{1/2}$ of mAbs Residualizing, signal retention in target tissues over time Low cost of production	Higher radiation exposure to normal organs than shorter-lived isotopes Residualizing, higher background signal in non-target tissues Labeling requires chelation, which can alter physiochemical properties of the probe
^{111}In	67.2 h	Requires SPECT, less expensive vs PET, multiplexing possible	Requires SPECT, less sensitive and lower spatial resolution vs PET
^{64}Cu	12.7 h	Suitable for use with Ab fragments and minibodies Widely available Residualizing, signal retention in target tissues over time Low cost of production Short positron range (high spatial resolution)	Low positron yield Increased patient radiation exposure due to β-particle and auger electron emission Labeling requires chelation, which can alter physiochemical properties of the probe Residualizing, higher background signal in non-target tissues High nonspecific uptake in liver
^{18}F	109.8 min	Widely available Ideal for labeling small molecules, peptides, adnectins, affibodies Lower radiation exposure to normal organs High positron yield Short positron range (high spatial resolution) Relative ease of on-site production	Cannot be used with larger molecule probes (eg, mAbs)
^{68}Ga	67 min	Ideal for labeling small molecules, peptides, adnectins, affibodies Lower radiation exposure to normal organs High positron yield Relative ease of on-site production	Long positron range (lower spatial resolution)
^{11}C	20.4 min	Widely available Rapid nontarget tissue clearance Lower radiation exposure to normal organs High positron yield Relative ease of production	Ultrashort $t_{1/2}$ limits clinical utility, can only be used with small molecules

Abbreviations: mAb = monoclonal antibody; PET = positron emission tomography; SPECT = single-photon emission computed tomography.

design of future trials using PD-L1 immuno-PET to optimize synergistic treatment regimens. For example, following the notion that intratumoral expression of immunosuppressive molecules, such as PD-L1, indicates the presence of pre-existing (albeit suppressed) T cell infiltrates that are a requisite factor for ICI reponses,[78] it may be possible for PD-L1 PET to differentiate these immunologically "hot" lesions from noninfiltrated "cold" lesions that are likely to be ICI-resistant. PET images could then guide radiation therapy targeting of cold lesions to trigger de novo inflammation and T cell infiltration to potentiate checkpoint blockade immunotherapy.

Antibody-based tracers have several advantages for immunoPET, including high antigen avidity and specificity needed to maximize signal-to-background ratios for visualizing PD-L1 within the TME. Using mouse/human cross-reactive mabs, which are already approved for use in humans, such as atezolizumab, also presents fewer challenges and safety hurdles for clinical translation than novel probes. However, antibodies also have inherent limitations that can hinder clinical utility. One disadvantage is their relatively high molecular weight and slow hepatic clearance, typically over days to weeks. Their large size also impedes rapid tumor penetration and

Table 4 Overview of select immunoPET tracers with clinical applications in cancer immunotherapy

Probe type	Optimal imaging time P.i.	Advantages	Limitations	Examples target tracer (published reference or Clinicaltrials.gov ID)	
Whole mAb ~150 kDa	5-7 d	Long $t_{1/2}$ of ^{89}Zr matches circulating $t_{1/2}$ of mAbs Ease of translation, can be produced from widely available, clinically approved mAbs High antigen specificity and avidity Relative ease of radiolabeling	Same-day infusion/imaging not possible due to slow clearance from nontarget tissues Not optimal for intracellular target epitopes Generally require coinfusion with unlabeled Ab to reduce tracer sequestration in antigen-sinks Low solid-tumor penetration	PD-L 1	^{89}Zr-Atezolizumab[102] ^{89}Zr-Atezolizumab (NCT04564482, opened Sept 2020) ^{89}Zr-Durvalumab[103,135] ^{89}Zr-Avelumab (NCT03514719, opened May 2018) ^{89}Zr-DFO-REGN3504 (NCT03746704, opened Nov 2018)
				PD-1	^{89}Zr-Pembrolizumab[136,137] ^{89}Zr-Nivolumab[104] ^{64}Cu-DOTA-Pembrolizumab (NCT04605614, opened October 2020)
				CD-8	^{89}ZED88082A[121]
				CTLA-4	^{89}Zr-Ipilimumab (NCT03313323, opened October 2017)
Probody ~150 kDa	7 d	High tumor specificity, lower uptake in nontumor lymphoid tissues vs Abs	Not widely accessible for routine clinical use	PD-L1	^{89}Zr-CX-072[108]
Antibody fragments (Fab, F(ab')$_2$, scFv) 25-100 kDa	4-48 h	Easily produced from intact abs Do not interact with Fc receptors Higher tumor-to background ratio vs intact abs Potential for same-day infusion/imaging Better solid tumor penetration vs intact abs	More difficult to radiolabel vs intact abs High nontarget accumulation in kidneys Lower tumor uptake vs intact abs	PD-L1	^{64}Cu-NOTA-αPD-L1 Fab[85] ^{89}Zr-Df-F(ab')$_2$[84] ^{89}Zr-C4 scFv[86]
				CTLA-4	^{64}Cu-NOTA-ipilimumab-F(ab')$_2$[138]

(*continued on next page*)

Table 4 (*Continued*)

Probe type	Optimal imaging time P.i.	Advantages	Limitations	Examples target tracer (published reference or Clinicaltrials.gov ID)	
Minibody, HcAb 80 kDa	5-24 h	Do not interact with Fc receptors Higher tumor-to background ratio vs intact abs Potential for same-day infusion/imaging	Not widely accessible for routine clinical use	PD-L1 CD-8	^{89}Zr-KN035 (NCT04977128, opened July 2021) ^{89}Zr-IAB22M2C[120,139] (NCT03802123, opened January 2019) ^{89}Zr-Df-Crefmirlimab (NCT05013099, opened Aug 2021)
Nanobody 15 kDa	60 min	Same-day infusion/imaging High tumor penetration High tumor-to-background ratio	High nontarget accumulation in kidneys Not widely accessible for routine clinical use	PD-L1 CD-8	^{68}Ga-NOTA-Nb109[87-89] ^{68}Ga-THP-APN09 (NCT05156515, opened December 2021) ^{68}Ga-NOTA-SNA006a[119] ^{68}Ga-NODAGA-SNA006 (NCT05126927, opened Nov 2021)
Small proteins ~10-15 kDa	60-90 min	Same-day infusion/imaging High tumor penetration	High nontarget accumulation in kidneys Not widely accessible for routine clinical use	PD-L1	^{18}F-BMS-986192[104,105,106] ^{68}Ga-DOTA-HACA-PD1[100]
Small peptides ~2-7 kDa	60 min	Same-day *infusion/imaging High tumor penetration	High nontarget accumulation in kidneys Not widely accessible for routine clinical use	PD-L1	^{68}Ga-WL12[107]

Abbreviations: Fab = antigen-binding fragment; HcAb = heavy-chain only antibody; mAb = monoclonal antibody; PD-L1 = programmed death-ligand 1; PET = positron emission tomography; P.i. = posttracer infusion; scFv = single-chain variable fragment.

distribution.[79,80] Long circulation times and slow tumor uptake prolong the time for tumor SUV_{max} and tumor-to-background ratio to stabilize, obligating patients to return several days after tracer infusion for imaging.[81,82] The intact Fc region and FcγR-binding capacity of certain IgG probes such as avelumab can also contribute to nonspecific uptake and high background signal, and can mediate unintended T cell depletion.[83]

These considerations led some investigators to design alternative tracers using nonwhole antibody moieties (Table 4). Preclinical studies have demonstrated the feasibility of using radiolabeled antibody fragments [Fab and $F(ab')_2$, single chain variable fragments (scFv), and minibodies[84-86]], nanobodies,[87-90] and smaller protein scaffolds (affibodies,[91,92] adnectins,[93,94] small protein binders,[95] peptides[96-99]) to detect PD-L1 expression. These small molecular weight probes are more rapidly cleared, which may be preferred for ease of clinical workflow (eg, same-day infusion and imaging) and short-interval serial monitoring. However, the shorter biological half-lives of such probes also reduce absolute tumor uptake, although this may be at least partially offset by lower uptake in normal tissues.[96,100]

Another recently investigated strategy to limit on-target-off-tumor uptake is with use of a "probody"-based tracer, designed to be preferentially activated and able to bind its target in the TME, while remaining inactive in normal tissues. Giesen et al[101] engineered the mouse/human cross-reactive anti-PD-L1 probody CX-072, an IgG-4 mAb with binding regions masked by a peptide that is removed in vivo by proteases. They showed that ^{89}Zr-CX-072 specifically accumulated in PD-L1-expressing syngeneic mouse tumors and human tumor xenografts, with comparatively low uptake in PD-L1 expressing normal tissues. An early phase clinical trial (NCT03013491) is currently in progress to evaluate this probody for therapeutic use in cancer patients. Altogether, these preclinical data provided a framework for initial clinical studies of PD-L1 PET in patients with cancer and highlight the potential of noninvasive molecular imaging to elucidate mechanisms of synergy between radiation and immunotherapy.

From mice to men: Early and ongoing clinical trials of PD-L1 immunoPET

The first human imaging studies have largely used radiolabeled therapeutic antibodies. Bensch et al[102] reported on the first-in-human PD-L1 PET study with ^{89}Zr-atezolizumab in patients with advanced NSCLC, bladder cancer, or triple-negative breast cancer, before atezolizumab monotherapy. They administered the tracer (coinfused with unlabeled mAb) to 22 ICI-naïve patients, followed by up to 4 PET/CT scans at 0 to 7 days postinfusion. Tumor-to-background ratios stabilized at day 7 postinfusion. Low tracer uptake was found in most normal tissues, apart from high uptake in lymph nodes and spleen and moderate uptake in bone marrow, compatible with target-specific binding on immune cells and endothelial littoral cells lining venous sinusoids. High tracer uptake was observed in a majority of tumors, although heterogeneous tracer distribution within individual lesions, as well as within-patient SUVmax heterogeneity in patients with multiple lesions, were also noted. Notably, ^{89}Zr-atezolizumab tumor uptake was a strong predictor of patient response to atezolizumab therapy; those with complete response showed a 235% higher tumor uptake (mean maximum standardized uptake value [SUV_{max}]) than patients who immediately progressed. Moreover, tumor uptake was strongly related to PFS and OS, as patients with below-median uptake were more likely to progress or die than those with above-median uptake (subset median of 9 SUV). In contrast, PD-L1 IHC on tumor biopsies (using 2 standardized assays) showed moderate to poor discrimination for patient outcome. This was both predictive and prognostic.

Smit et al[103] recently reported on the safety and feasibility of another ^{89}Zr-labeled anti-PD-L1 mAb, durvalumab, in 10 ICI-naïve patients with advanced NSCLC. In this study, patients received the first administration of tracer without coinfusion of unlabeled antibody and underwent PET scan at 120 hours postinfusion. After a 12-day wash-out period, patients received a second ^{89}Zr-durvalumab dose, coadministered with a therapeutic dose of unlabeled durvalumab. As in the aforementioned study with ^{89}Zr-atezolizumab, high uptake of ^{89}Zr-durvalumab was similarly observed in the spleen and moderate uptake in bone marrow, as well as high uptake in the liver attributed to tracer catabolism. Heterogenous uptake was observed in larger tumors, highest in the periphery of the tumor, which the authors postulated could be due to impaired vascularization, barrier effect, or a higher prevalence of PD-L1 expressing immune cells at the tumor periphery. As expected, imaging performed after coadministered tracer/unlabeled mAb revealed much lower uptake in all target tissues including tumors, compared with the tracer-only scans. This was attributed to saturation of PD-L1 receptors by the much higher therapeutic dose (750 mg) compared with tracer dose (2 mg). Notably, fewer PD-L1 positive lesions overall were identifiable in the second scan series, possibly suggesting that PD-L1 positive tumors with low-to-moderate expression were saturated with unlabeled antibody and were unable to bind sufficient tracer to be delineable. However, in one case, a large well-vascularized tumor in the lung was not well visualized on the first imaging series yet showed significant uptake in the second series. This example supports the idea that coinfusion with unlabeled antibody permits a larger fraction of tracer to remain in the blood pool, available for uptake by PD-L1 high tumors. These

conflicting observations imply that coinfusion with a full therapeutic dose may be a suboptimal strategy for assessing PD-L1 expression status in the clinical context, as strong responses to PD-1/PD-L1 inhibitors are frequently observed in patients with low-to-moderate PD-L1 expression by IHC. In this pilot study's limited patient cohort, nonsignificant correlations were observed between clinical outcome with durvalumab therapy and tracer uptake. Future trials should explore the effect of unlabeled carrier dose on PD-L1 PET sensitivity and specificity in various patient populations.

Immuno-PET with non-IgG low-molecular weight probes has also early promise in patients.[104-107] As mentioned, an advantage of these smaller probes over antibody-based tracers is their rapid clearance kinetics, permitting same-day infusion and imaging, and favorable target-to-background contrast. Niemeijer et al[104] demonstrated that PET imaging with ^{18}F-BMS-986192, a fluorinated anti-PD-L1 adnectin, can be performed as soon as 1 hour after tracer infusion for semiquantitative evaluation of tumor PD-L1 expression in patients with advanced NSCLC. In this study, patients also underwent subsequent immuno-PET with ^{89}Zr-nivolumab, followed by nivolumab monotherapy. Lesions determined to be PD-L1-positive by IHC and ^{18}F-BMS-986192 PET were observed to accumulate ^{89}Zr-nivolumab, supporting the presumption that therapeutic nivolumab works to block PD-1/PD-L1 pathway signaling within tumors that have co-opted the pathway for immune escape. Furthermore, uptake of both tracers was reported to predict lesion-level response to nivolumab. Nienhuis et al[106] found similar predictive capacity of ^{18}F-BMS-986192 PET melanoma metastases, and furthermore, that it may be able to identify PD-L1-expressing brain metastases in some patients. The utility of ^{18}F-BMS-986192 PET in additional patient populations is currently being explored (NCT03843515, 2018-000462-11).

Using another high-affinity PD-L1-binding small peptide probe (WL12), labeled with ^{68}Ga, Zhou et al[107] also showed feasibility of same-day immunoPET.[107] Nine treatment-naïve patients with NSCLC with PD-L1-positivity by IHC underwent PET/CT at 1 to 2 hours after tracer infusion. Significant intra- and intertumoral heterogeneity in uptake was noted in some patients, and tumor SUV_{max} strongly correlated with PD-L1 IHC results. Although only 3 patients went on to receive PD-1 directed therapy, clinical outcomes for all 3 correlated with tracer uptake.

Lastly, building on the encouraging preclinical data for ^{89}Zr-CX-072 highlighted above, Ruijter et al[108] recently reported on results of a sub study investigating this probody for immuno-PET in patients with metastatic cancer. PET images obtained 2 to 7 days after infusion of ^{89}Zr-CX-072 showed tumor uptake in all patients, even in those who were reported as PD-L1-negative by IHC. In line with findings from studies using antibody-based tracers, heterogeneous uptake was observed within and between tumors, and high uptake of ^{89}Zr-CX-072 occurred in the spleen attributed to specific binding to PD-L1 expressing littoral cells, although this was partially mitigated with coinfusion of sufficient unlabeled protein dose. The study reported similar or lower uptake of ^{89}Zr-CX-072 in other healthy tissues, including nonmetastatic lymphoid organs, compared with prior findings with ^{89}Zr-atezolizumab, supporting tumor-associated protease activation of the probody. All 8 patients subsequently received CX-072 (monotherapy, with one patient additionally receiving ipilimumab), although results of the treatment study (NCT03013491) have not yet been reported.

CD8+ PET

Evaluation of PD-L1 expression in tumors is undoubtedly valuable for predicting responses to PD-1/PD-L1 blockade. However, PD-L1 is an imperfect biomarker, as evidenced by the observation that patients bearing PD-L1-positive tumors are not always responsive to anti-PD-1/PD-L1 antibodies. Although PD-L1 expression within tumors can be induced by immune-stimulating cytokines such as interferons released by activated T cells,[109] it can also be constitutively expressed by tumor cells associated with genetic alterations, in the absence of infiltrating immune cells or CD8+ T cell activation.[110,111] Given the complexity of PD-L1 expression regulation and potential multilayered immune tolerizing mechanisms hindering antitumor responses, molecular imaging of multiple immunologic biomarkers in addition to PD-L1 could provide more information about the state of the tumor-immune dynamic, with potential therapeutic implications.

Several studies have supported that PD-L1 expression in the tumor is most useful for predicting positive clinical outcomes to ICI therapy when it is observed in the context of an ongoing active T cell response.[42,112] The presence of tumor infiltrating dendritic cells, CD8+ T cells, cytokines such as granzyme B, and PD-L1 expression indicates an immunogenic (hot) phenotype, which is a prerequisite for anti-PD-1/PD-L1 therapy. In fact, the density of tumor infiltrating lymphocytes (TIL) positively correlates with clinical responses to various immunotherapies, including anti-PD-1/PD-L1 antibodies.[45,113,114] Ongoing research into ICI therapy resistance is focused on methods to effectively create an immunogenic TME within a nonimmunogenic (cold) tumor, that would then respond to checkpoint blockade.

Similar to PD-L1, tumor infiltration by CD8+ T cells has most frequently been evaluated via tissue-based methods, which are likewise subject to biologic and technical limitations. Thus, immunoPET using anti-CD8 antibody

probes is being explored as a method of visualizing CD8+ T cell trafficking and tumor infiltration.

Preclinical studies have demonstrated success of immunoPET for visualizing CD8+ T cell trafficking, and changes in tumor-infiltrating T cell densities after ICI therapy, using various antibody-based and nonantibody tracers.[115–119] Recently, phase 1 and 2 clinical trials have also shown early promise for 2 CD8 PET tracers (^{89}Zr-Df-IAB22M2C[120] and ^{89}Zr-ED88082A[121]), where intratumoral uptake correlated with clinical outcomes after ICI therapy. Going further, multiple immunoPET probes to evaluate intratumoral cytotoxic T cell effector function via granzyme B[122\] and interferon-y[123] have also been developed, although these strategies are yet to be explored in clinical trials.

Conclusions and Future Directions for Radiation Oncology

The use of molecular imaging techniques to evaluate immune system changes and predict clinical responses is still in its infancy. Along with the promising developments highlighted above, several challenges to must be considered before widespread clinical use of immunoPET can be realized. For one, ongoing and future prospective clinical trials will need to demonstrate that use of immunoPET for patient stratification and treatment planning results in equivalent or better patient outcomes than those achieved with current biomarkers and imaging modalities. As we discussed herein, we believe immunoPET overcomes many of the inherent limitations of PD-L1 IHC and conventional imaging techniques. Beyond establishment of clinical benefit, imaging protocols and interpretation methods for each novel tracer will need to be standardized and harmonized across multiple sites, as well as guidelines established for radiotracer production under good manufacturing practice conditions, ultimately to achieve FDA approval. However, the already well-established infrastructure for radiopharmaceutical production and distribution in many geographic areas can facilitate access to newly approved tracers at sites without regulatory approval for on-site production or access to a cyclotron. Finally, although commercial sources for radiotracers can help to reduce overall procedural costs, cost-effectiveness analyses will be critical to assess whether the additional benefits of these state-of-the-art imaging strategies justify the expenses associated with implementation and use. As we noted previously, many immune checkpoint inhibitor drugs are associated with substantial financial costs of ≥$150,000 annually. Therefore, we anticipate that PD-1/PD-L1 immunoPET will achieve cost-effectiveness by improving selection of patients most likely to respond to checkpoint inhibition.

ImmunoPET has potential for broad utility within the field of radiation oncology, particularly as evidence accumulates for radiation to potentiate the systemic antitumor effect of immunotherapies, and for immunotherapies to amplify the efficacy of targeted radiation therapy. Radiation can have a multitude of immune-mediated effects, resulting in both immune stimulation and immune suppression. The primary immunomodulatory effects within the TME in response to moderate-to-high dose radiation include induction of immunogenic cell death and release of tumor neoantigens, upregulation of major histocompatibility complex I, death receptors such as Fas, and PD-L1, leakage of DNA into the cytosol triggering activation of the cGAS/STING pathway and downstream TIL infiltration, as well as temporary local eradication of suppressor and effector lymphocytes, and delayed recruitment of suppressor T regulatory cells. As discussed above, radiation in combination with ICI therapy may be particularly useful for treating patients with immunologically “cold” tumors, due to these radiation-induced immune modifications within the TME.

Currently, an area of great clinical interest is elucidation of synergistic combinatorial strategies of radiation and immunotherapy. Numerous ongoing preclinical and clinical studies are exploring combined anti-PD-1/PD-L1 antibody therapy and radiation therapy regimens, with the goal to define optimal radiation dose, fractionation, target volume, and sequencing with immunotherapy. In these contexts, immunoPET could be used to stratify patients predicted to respond versus nonresponders and to characterize radiation-induced changes in PD-L1 expression and T cell infiltration, which will help to expand the proportion of patients who can benefit from ICI. Furthermore, akin to PSMA-based PET imaging for prostate cancer, immunoPET could be used to inform adjunct treatment planning and radiation target delineation; for example, in a patient with oligoprogression on ICI therapy, immunoPET might identify lesions with low PD-L1 expression and CD8+ T cell infiltration that could be turned “hot” with radiation therapy. Lastly, ImmunoPET using novel radiopharmaceutical tracers could also be used in future trials of other radiation-immunotherapy combination strategies, such as with chimeric antigen receptor T cell (CAR-T) therapies, IDO inhibitors, vaccines, and oncolytic viruses, to visualize complex immunologic changes within the TME in real-time. These considerations highlight the significant promise of immunoPET to improve personalized multimodality cancer treatment.

References

1. Hodi FS, O’Day SJ, McDermott DF, et al. Improved survival with ipilimumab in patients with metastatic melanoma. *N Engl J Med*. 2010;363:711–723.

2. Brahmer JR, Tykodi SS, Chow LQM, et al. Safety and activity of anti-PD-L1 antibody in patients with advanced cancer. *N Engl J Med*. 2012;366:2455–2465.
3. Powles T, Eder JP, Fine GD, et al. MPDL3280A (anti-PD-L1) treatment leads to clinical activity in metastatic bladder cancer. *Nature*. 2014;515:558–562.
4. Topalian SL, Hodi FS, Brahmer JR, et al. Safety, activity, and immune correlates of anti-PD-1 antibody in cancer. *N Engl J Med*. 2012;366:2443–2454.
5. Ribas A, Hamid O, Daud A, et al. Association of pembrolizumab with tumor response and survival among patients with advanced melanoma. *JAMA*. 2016;315:1600–1609.
6. Reck M, Rodríguez-Abreu D, Robinson AG, et al. Pembrolizumab versus Chemotherapy for PD-L1−positive non−small-cell lung cancer. *N Engl J Med*. 2016;375:1823–1833.
7. Twomey JD, Zhang B. Cancer immunotherapy update: FDA-approved checkpoint inhibitors and companion diagnostics. *AAPS J*. 2021;23:39.
8. Haslam A, Prasad V. Estimation of the percentage of US patients with cancer who are eligible for and respond to checkpoint inhibitor immunotherapy drugs. *JAMA Netw Open*. 2019;2: e192535.
9. Zhao B, Zhao H, Zhao J. Efficacy of PD-1/PD-L1 blockade monotherapy in clinical trials. *Ther Adv Med Oncol*. 2020;12: 1758835920937612.
10. Martins F, Sofiya L, Sykiotis GP, et al. Adverse effects of immune-checkpoint inhibitors: epidemiology, management and surveillance. *Nat Rev Clin Oncol*. 2019;16:563–580.
11. Sezen D, Verma V, He K, et al. Considerations for clinical trials testing radiotherapy combined with immunotherapy for metastatic disease. *Semin Radiat Oncol*. 2021;31:217–226.
12. Melero I, Berman DM, Aznar MA, Korman AJ, Gracia JLP, Haanen J. Evolving synergistic combinations of targeted immunotherapies to combat cancer. *Nat Rev Cancer*. 2015;15:457–472.
13. Welsh J, Menon H, Chen D, et al. Pembrolizumab with or without radiation therapy for metastatic non-small cell lung cancer: A randomized phase I/II trial. *J Immunother Cancer*. 2020;8: e001001.
14. Cushman TR, Caetano MS, Welsh JW, Verma V. Overview of ongoing clinical trials investigating combined radiotherapy and immunotherapy. *Immunotherapy*. 2018;10:851.. -850.
15. Chen D, Menon H, Verma V, et al. Response and outcomes after anti-CTLA4 versus anti-PD1 combined with stereotactic body radiation therapy for metastatic non-small cell lung cancer: Retrospective analysis of 2 single-institution prospective trials. *J Immunother Cancer*. 2020;8: e000492.
16. Patel SP, Kurzrock R. PD-L1 expression as a predictive biomarker in cancer immunotherapy. *Mol Cancer Ther*. 2015;14:847–856.
17. Hofman MS, Lawrentschuk N, Francis RJ, et al. Prostate-specific membrane antigen PET-CT in patients with high-risk prostate cancer before curative-intent surgery or radiotherapy (proPSMA): A prospective, randomised, multicentre study. *Lancet Lond Engl*. 2020;395:1208–1216.
18. Phillips R, Shi WY, Deek M, et al. Outcomes of observation vs stereotactic ablative radiation for oligometastatic prostate cancer: The ORIOLE phase 2 randomized clinical trial. *JAMA Oncol*. 2020;6:650–659.
19. Jubel JM, Barbati ZR, Burger C, Wirtz DC, Schildberg FA. The role of PD-1 in acute and chronic infection. *Front Immunol*. 2020;11:487.
20. Dai X, Gao Y, Wei W. Posttranslational regulations of PD-L1 and PD-1: Mechanisms and opportunities for combined immunotherapy. *Semin Cancer Biol*. 2022. https://doi.org/10.1016/j.semcancer.2021.04.002. [e-pub ahead of print]. Accessed December 11, 2021.
21. Wherry EJ, Kurachi M. Molecular and cellular insights into T cell exhaustion. *Nat Rev Immunol*. 2015;15:486–499.
22. Seliger B. Basis of PD1/PD-L1 therapies. *J Clin Med*. 2019;8:2168.
23. Qin W, Hu L, Zhang X, et al. The diverse function of PD-1/PD-L pathway beyond cancer. *Front Immunol*. 2019;10:2298.
24. Hudson K, Cross N, Jordan-Mahy N, Leyland R. The extrinsic and intrinsic roles of PD-L1 and its receptor PD-1: Implications for immunotherapy treatment. *Front Immunol*. 2020;11:2362.
25. US Food and Drug Administration. List of cleared or approved companion diagnostic devices (in vitro and imaging tools). Published December 1, 2021. Available at: https://www.fda.gov/medical-devices/in-vitro-diagnostics/list-cleared-or-approved-companion-diagnostic-devices-in-vitro-and-imaging-tools.
26. Garon EB, Rizvi NA, Hui R, et al. Pembrolizumab for the treatment of non−small-cell lung cancer. *N Engl J Med*. 2015;372:2018–2028.
27. Herbst RS, Baas P, Kim DW, et al. Pembrolizumab versus docetaxel for previously treated, PD-L1-positive, advanced non-small-cell lung cancer (KEYNOTE-010): A randomised controlled trial. *The Lancet*. 2016;387:1540–1550.
28. Daud AI, Wolchok JD, Robert C, et al. Programmed death-ligand 1 expression and response to the anti-programmed death 1 antibody pembrolizumab in melanoma. *J Clin Oncol*. 2016;34:4102–4109.
29. Robert C, Schachter J, Long GV, et al. Pembrolizumab versus ipilimumab in advanced melanoma. *N Engl J Med*. 2015;372:2521–2532.
30. Grosso J, Horak CE, Inzunza D, et al. Association of tumor PD-L1 expression and immune biomarkers with clinical activity in patients (pts) with advanced solid tumors treated with nivolumab (anti-PD-1; BMS-936558; ONO-4538). *J Clin Oncol*. 2013;31(15 Suppl):3016.
31. Rittmeyer A, Barlesi F, Waterkamp D, et al. Atezolizumab versus docetaxel in patients with previously treated non-small-cell lung cancer (OAK): A phase 3, open-label, multicentre randomised controlled trial. *The Lancet*. 2017;389:255–265.
32. Bellmunt J, De Wit R, Vaughn DJ, et al. Pembrolizumab as second-line therapy for advanced urothelial carcinoma. *N Engl J Med*. 2017;376:1015–1026.
33. Carbone DP, Reck M, Paz-Ares L, et al. *First-line nivolumab in stage IV or recurrent non−small-cell lung cancer*. 2017;376:2415–2426.
34. Balar AV, Galsky MD, Rosenberg JE, et al. Atezolizumab as first-line treatment in cisplatin-ineligible patients with locally advanced and metastatic urothelial carcinoma: A single-arm, multicentre, phase 2 trial. *Lancet Lond Engl*. 2017;389:67–76.
35. Sharma P, Callahan MK, Bono P, et al. Nivolumab monotherapy in recurrent metastatic urothelial carcinoma (CheckMate 032): A multicentre, open-label, phase 1/2 trial. *Lancet Oncol*. 2016;17:1590–1598.
36. Hirsch FR, McElhinny A, Stanforth D, et al. PD-L1 immunohistochemistry assays for lung cancer: Results from phase 1 of the blueprint PD-L1 IHC assay comparison project. *J Thorac Oncol*. 2017;12:208–222.
37. Tsao MS, Kerr KM, Kockx M, et al. PD-L1 immunohistochemistry comparability study in real-life clinical samples: Results of blueprint phase 2 project. *J Thorac Oncol*. 2018;13:1302–1311.
38. Brunnström H, Johansson A, Westbom-Fremer S, et al. PD-L1 immunohistochemistry in clinical diagnostics of lung cancer: Inter-pathologist variability is higher than assay variability. *Mod Pathol*. 2017;30:1411–1421.
39. Herbst RS, Baas P, Perez-Gracia JL, et al. Use of archival versus newly collected tumor samples for assessing PD-L1 expression and overall survival: An updated analysis of KEYNOTE-010 trial. *Ann Oncol*. 2019;30:281–289.
40. Hofman P. The challenges of evaluating predictive biomarkers using small biopsy tissue samples and liquid biopsies from non-small cell lung cancer patients. *J Thorac Dis*. 2019;11(Suppl 1):S57–S64.
41. Kluger HM, Zito CR, Turcu G, et al. PD-L1 studies across tumor types, its differential expression and predictive value in patients

treated with immune checkpoint inhibitors. *Clin Cancer Res*. 2017;23:4270–4279.
42. Madore J, Vilain RE, Menzies AM, et al. PD-L1 expression in melanoma shows marked heterogeneity within and between patients: Implications for anti-PD-1/PD-L1 clinical trials. *Pigment Cell Melanoma Res*. 2015;28:245–253.
43. McLaughlin J, Han G, Schalper KA, et al. Quantitative assessment of the heterogeneity of PD-L1 expression in non-small-cell lung cancer. *JAMA Oncol*. 2016;2:46–54.
44. Martelotto LG, Ng CK, Piscuoglio S, Weigelt B, Reis-Filho JS. Breast cancer intra-tumor heterogeneity. *Breast Cancer Res*. 2014;16:210.
45. Sharma P, Allison JP. The future of immune checkpoint therapy. *Science*. 2015;348:56–61.
46. Twyman-Saint Victor C, Rech AJ, Maity A, et al. Radiation and dual checkpoint blockade activate nonredundant immune mechanisms in cancer. *Nature*. 2015;520:373–377.
47. Munari E, Zamboni G, Marconi M, et al. PD-L1 expression heterogeneity in non-small cell lung cancer: Evaluation of small biopsies reliability. *Oncotarget*. 2017;8:90123–90131.
48. Munari E, Zamboni G, Lunardi G, et al. PD-L1 expression heterogeneity in non−small cell lung cancer: Defining criteria for harmonization between biopsy specimens and whole sections. *J Thorac Oncol*. 2018;13:1113–1120.
49. Wolchok JD, Hoos A, O'Day S, et al. Guidelines for the evaluation of immune therapy activity in solid tumors: Immune-related response criteria. *Clin Cancer Res*. 2009;15:7412–7420.
50. Nishino M, Gargano M, Suda M, Ramaiya NH, Hodi FS. Optimizing immune-related tumor response assessment: Does reducing the number of lesions impact response assessment in melanoma patients treated with ipilimumab? *J Immunother Cancer*. 2014;2:17.
51. Hodi FS, Ballinger M, Lyons B, et al. Immune-Modified Response Evaluation Criteria In Solid Tumors (imRECIST): Refining guidelines to assess the clinical benefit of cancer immunotherapy. *J Clin Oncol*. 2018;36:850–858.
52. Gillies RJ, Kinahan PE, Hricak H. Radiomics: Images are more than pictures, they are data. *Radiology*. 2016;278:563–577.
53. Tang C, Hobbs B, Amer A, et al. Development of an immune-pathology informed radiomics model for non-small cell lung cancer. *Sci Rep*. 2018;8:1922.
54. Tunali I, Gray JE, Qi J, et al. Novel clinical and radiomic predictors of rapid disease progression phenotypes among lung cancer patients treated with immunotherapy: An early report. *Lung Cancer*. 2019;129:75–79.
55. Kohutek ZA, Wu AJ, Zhang Z, et al. FDG-PET maximum standardized uptake value is prognostic for recurrence and survival after stereotactic body radiotherapy for non-small cell lung cancer. *Lung Cancer*. 2015;89:115–120.
56. Gregory DL, Hicks RJ, Hogg A, et al. Effect of PET/CT on management of patients with non-small cell lung cancer: Results of a prospective study with 5-year survival data. *J Nucl Med*. 2012;53:1007–1015.
57. Shepherd T, Teras M, Beichel RR, et al. Comparative study with new accuracy metrics for target volume contouring in PET image guided radiation therapy. *IEEE Trans Med Imaging*. 2012;31:2006–2024.
58. Wahl RL, Jacene H, Kasamon Y, Lodge MA. From RECIST to PERCIST: Evolving considerations for PET response criteria in solid tumors. *J Nucl Med*. 2009;50(Suppl 1):122S–150S.
59. Kaira K, Higuchi T, Naruse I, et al. Metabolic activity by 18F-FDG-PET/CT is predictive of early response after nivolumab in previously treated NSCLC. *Eur J Nucl Med Mol Imaging*. 2018;45:56–66.
60. Chardin D, Paquet M, Schiappa R, et al. Baseline metabolic tumor volume as a strong predictive and prognostic biomarker in patients with non-small cell lung cancer treated with PD1 inhibitors: A prospective study. *J Immunother Cancer*. 2020;8: e000645.
61. Cho SY, Lipson EJ, Im HJ, et al. Prediction of response to immune checkpoint inhibitor therapy using early-time-point ^{18}F-FDG PET/CT imaging in patients with advanced melanoma. *J Nucl Med*. 2017;58:1421–1428.
62. Grizzi F, Castello A, Lopci E. Is it time to change our vision of tumor metabolism prior to immunotherapy? *Eur J Nucl Med Mol Imaging*. 2018;45:1072–1075.
63. Heskamp S, Hobo W, Molkenboer-Kuenen JDM, et al. Noninvasive imaging of tumor PD-L1 expression using radiolabeled anti−PD-L1 Antibodies. *Cancer Res*. 2015;75:2928–2936.
64. Kikuchi M, Clump DA, Srivastava RM, et al. Preclinical immuno-PET/CT imaging using Zr-89-labeled anti-PD-L1 monoclonal antibody for assessing radiation-induced PD-L1 upregulation in head and neck cancer and melanoma. *Oncoimmunology*. 2017;6: e1329071.
65. Chatterjee S, Lesniak WG, Gabrielson M, et al. A humanized antibody for imaging immune checkpoint ligand PD-L1 expression in tumors. *Oncotarget*. 2016;7:10215–10227.
66. Hettich M, Braun F, Bartholomä MD, Schirmbeck R, Niedermann G. High-resolution PET imaging with therapeutic antibody-based PD-1/PD-L1 checkpoint tracers. *Theranostics*. 2016;6:1629–1640.
67. Lesniak WG, Chatterjee S, Gabrielson M, et al. PD-L1 Detection in tumors using [64Cu]atezolizumab with PET. *Bioconjug Chem*. 2016;27:2103–2110.
68. Moroz A, Lee CY, Wang YH, et al. A preclinical assessment of 89Zr-atezolizumab identifies a requirement for carrier added formulations not observed with 89Zr-C4. *Bioconjug Chem*. 2018;29:3476–3482.
69. Josefsson A, Nedrow JR, Park S, et al. Imaging, biodistribution, and dosimetry of radionuclide-labeled pD-L1 antibody in an immunocompetent mouse model of breast cancer. *Cancer Res*. 2016;76:472–479.
70. Nedrow JR, Josefsson A, Park S, Ranka S, Roy S, Sgouros G. Imaging of programmed cell death ligand 1: Impact of protein concentration on distribution of anti-PD-L1 SPECT agents in an immunocompetent murine model of melanoma. *J Nucl Med*. 2017;58:1560–1566.
71. Pang X, Liu M, Wang R, Liao X, Yan P, Zhang C. Radioimmunoimaging and targeting treatment in an immunocompetent murine model of triple-negative breast cancer using radiolabeled antiprogrammed death-ligand 1 monoclonal antibody. *J Label Compd Radiopharm*. 2018;61:826–836.
72. Jagoda EM, Vasalatiy O, Basuli F, et al. Immuno-PET imaging of the programmed cell death-1 ligand (PD-L1) using a zirconium-89 labeled therapeutic antibody, avelumab. *Mol Imaging*. 2019;18: 1536012119829986.
73. Ehlerding EB, Lee HJ, Barnhart TE, et al. Noninvasive imaging and quantification of radiotherapy-induced PD-L1 upregulation with 89Zr−Df−atezolizumab. *Bioconjug Chem*. 2019;30:1434–1441.
74. Christensen C, Kristensen LK, Alfsen MZ, Nielsen CH, Kjaer A. Quantitative PET imaging of PD-L1 expression in xenograft and syngeneic tumour models using a site-specifically labelled PD-L1 antibody. *Eur J Nucl Med Mol Imaging*. 2020;47:1302–1313.
75. Zhao J, Wen X, Li T, et al. Concurrent injection of unlabeled antibodies allows positron emission tomography imaging of programmed cell death ligand 1 expression in an orthotopic pancreatic tumor model. *ACS Omega*. 2020;5:8474–8482.
76. Centanni M, Moes DJAR, Trocóniz IF, Ciccolini J, van Hasselt JGC. Clinical pharmacokinetics and pharmacodynamics of immune checkpoint inhibitors. *Clin Pharmacokinet*. 2019;58:835–857.
77. Yoon JK, Park BN, Ryu EK, An YS, Lee SJ. Current perspectives on 89Zr-PET imaging. *Int J Mol Sci*. 2020;21:4309.
78. Gajewski TF, Corrales L, Williams J, Horton B, Sivan A, Spranger S. Cancer immunotherapy targets based on understanding the T

cell-inflamed versus non-T cell-inflamed tumor microenvironment. *Adv Exp Med Biol*. 2017;1036:19–31.
79. Lee CM, Tannock IF. The distribution of the therapeutic monoclonal antibodies cetuximab and trastuzumab within solid tumors. *BMC Cancer*. 2010;10:255.
80. Wittrup KD, Thurber GM, Schmidt MM, Rhoden JJ. Chapter ten: Practical theoretic guidance for the design of tumor-targeting agents. In: Wittrup KD, Verdine GL, eds. Methods in Enzymology, *vol 503*. Protein Engineering for Therapeutics, Part B. Cambridge, MA: Academic Press; 2012:255–268.
81. Thurber GM, Schmidt MM, Wittrup KD. Antibody tumor penetration: Transport opposed by systemic and antigen-mediated clearance. *Adv Drug Deliv Rev*. 2008;60:1421–1434.
82. Wilks MQ, Knowles SM, Wu AM, Huang SC. Improved modeling of in vivo kinetics of slowly diffusing radiotracers for tumor imaging. *J Nucl Med*. 2014;55:1539–1544.
83. Maute RL, Gordon SR, Mayer AT, et al. Engineering high-affinity PD-1 variants for optimized immunotherapy and immuno-PET imaging. *Proc Natl Acad Sci*. 2015;112:E6506–E6514.
84. Bridgwater C, Geller A, Hu X, et al. 89Zr-labeled anti-PD-L1 antibody fragment for evaluating in vivo PD-L1 levels in melanoma mouse model. *Cancer Biother Radiopharm*. 2020;35:549–557.
85. Wissler HL, Ehlerding EB, Lyu Z, et al. Site-specific immuno-PET tracer to image PD-L1. *Mol Pharm*. 2019;16:2028–2036.
86. Wei J, Wang Y hua, Lee CY, et al. An analysis of isoclonal antibody formats suggests a role for measuring PD-L1 with low molecular weight PET radiotracers. *Mol Imaging Biol*. 2020;22:1553–1561.
87. Lv G, Sun X, Qiu L, et al. PET imaging of tumor PD-L1 expression with a highly specific nonblocking single-domain antibody. *J Nucl Med*. 2020;61:117–122.
88. Qin S, Yu Y, Guan H, et al. A preclinical study: Correlation between PD-L1 PET imaging and the prediction of therapy efficacy of MC38 tumor with 68Ga-labeled PD-L1 targeted nanobody. *Aging*. 2021;13:13006–13022.
89. Liu Q, Jiang L, Li K, et al. Immuno-PET imaging of 68Ga-labeled nanobody Nb109 for dynamic monitoring the PD-L1 expression in cancers. *Cancer Immunol Immunother CII*. 2021;70:1721–1733.
90. Jiang J, Zhang M, Li G, et al. Evaluation of 64Cu radiolabeled antihPD-L1 Nb6 for positron emission tomography imaging in lung cancer tumor mice model. *Bioorg Med Chem Lett*. 2020;30:126915.
91. Trotter DEG, Meng X, McQuade P, et al. In vivo imaging of the programmed death ligand 1 by 18F PET. *J Nucl Med*. 2017;58:1852–1857.
92. Rubins DJ, Meng X, McQuade P, et al. In vivo evaluation and dosimetry estimate for a high affinity affibody PET tracer targeting PD-L1. *Mol Imaging Biol*. 2021;23:241–249.
93. Donnelly DJ, Smith RA, Morin P, et al. Synthesis and biologic evaluation of a novel 18F-labeled adnectin as a PET radioligand for imaging PD-L1 expression. *J Nucl Med*. 2018;59:529–535.
94. Robu S, Richter A, Gosmann D, et al. Synthesis and preclinical evaluation of a 68Ga-labeled adnectin, 68Ga-BMS-986192, as a PET agent for imaging PD-L1 expression. *J Nucl Med*. 2021;62:1228–1234.
95. Natarajan A, Patel CB, Ramakrishnan S, Panesar PS, Long SR, Gambhir SS. A novel engineered small protein for positron emission tomography imaging of human programmed death ligand-1: Validation in mouse models and human cancer tissues. *Clin Cancer Res*. 2019;25:1774–1785.
96. Chatterjee S, Lesniak WG, Miller MS, et al. Rapid PD-L1 detection in tumors with PET using a highly specific peptide. *Biochem Biophys Res Commun*. 2017;483:258–263.
97. De Silva RA, Kumar D, Lisok A, et al. Peptide-based 68Ga-PET radiotracer for imaging PD-L1 expression in cancer. *Mol Pharm*. 2018;15:3946–3952.
98. Kumar D, Lisok A, Dahmane E, et al. Peptide-based PET quantifies target engagement of PD-L1 therapeutics. *J Clin Invest*. 2022;129:616–630.
99. Lesniak WG, Mease RC, Chatterjee S, et al. Development of [18F] FPy-WL12 as a PD-L1 Specific PET Imaging Peptide. *Mol Imaging*. 2019;18: 1536012119852189.
100. Mayer AT, Natarajan A, Gordon SR, et al. Practical immuno-PET radiotracer design considerations for human immune checkpoint imaging. *J Nucl Med*. 2017;58:538–546.
101. Giesen D, Broer LN, de Hooge MNL, et al. Probody therapeutic design of 89Zr-CX-072 promotes accumulation in PD-L1 −expressing tumors compared to normal murine lymphoid tissue. *Clin Cancer Res*. 2020;26:3999–4009.
102. Bensch F, van der Veen EL, Lub-de Hooge MN, et al. 89Zr-atezolizumab imaging as a noninvasive approach to assess clinical response to PD-L1 blockade in cancer. *Nat Med*. 2018;24:1852–1858.
103. Smit J, Borm FJ, Niemeijer ALN, et al. PD-L1 PET/CT imaging with radiolabeled durvalumab in patients with advanced stage non-small cell lung cancer. *J Nucl Med*. 2022. https://doi.org/10.2967/jnumed.121.262473. [e-pub ahead of print]. Accessed January 22, 2022.
104. Niemeijer AN, Leung D, Huisman MC, et al. Whole body PD-1 and PD-L1 positron emission tomography in patients with non-small-cell lung cancer. *Nat Commun*. 2018;9:4664.
105. Huisman MC, Niemeijer ALN, Windhorst AD, et al. Quantification of PD-L1 expression with ^{18} F-BMS-986192 PET/CT in patients with advanced-stage non−small cell lung cancer. *J Nucl Med*. 2020;61:1455–1460.
106. Nienhuis PH, Antunes IF, Glaudemans AWJM, et al. ^{18}F-BMS986192 PET imaging of PD-L1 in metastatic melanoma patients with brain metastases treated with immune checkpoint inhibitors. A pilot study. *J Nucl Med*. 2022. https://doi.org/10.2967/jnumed.121.262368. [e-pub ahead of print]. Accessed January 22, 2022.
107. Zhou X, Jiang J, Yang X, et al. First-in-human evaluation of a PD-L1-binding peptide radiotracer in non-small cell lung cancer patients with PET. *J Nucl Med*. 2022;63:536–542.
108. de Ruijter LK, JS Hooiveld-Noeken, Giesen D, et al. First-in-human study of the biodistribution and pharmacokinetics of 89Zr-CX-072, a novel immunopet tracer based on an anti−PD-L1 probody. *Clin Cancer Res*. 2021;27:5325–5333.
109. Dong H, Strome SE, Salomao DR, et al. Tumor-associated B7-H1 promotes T-cell apoptosis: A potential mechanism of immune evasion. *Nat Med*. 2002;8:793–800.
110. Lastwika KJ, Wilson W, Li QK, et al. Control of PD-L1 expression by oncogenic activation of the AKT-mTOR pathway in non-small cell lung cancer. *Cancer Res*. 2016;76:227–238.
111. Ansell SM, Lesokhin AM, Borrello I, et al. *PD-1 blockade with nivolumab in relapsed or refractory Hodgkin's lymphoma*. 2015;372:311–319.
112. Tumeh PC, Harview CL, Yearley JH, et al. PD-1 blockade induces responses by inhibiting adaptive immune resistance. *Nature*. 2014;515:568–571.
113. Trujillo JA, Sweis RF, Bao R, Luke JJ. T cell−inflamed versus non-T cell−inflamed tumors: conceptual framework for cancer immunotherapy drug development and combination therapy selection. *Cancer Immunol Res*. 2018;6:990–1000.
114. Fridman WH, Pagès F, Sautès-Fridman C, Galon J. The immune contexture in human tumours: Impact on clinical outcome. *Nat Rev Cancer*. 2012;12:298–306.
115. Seo JW, Tavaré R, Mahakian LM, et al. CD8+ T-cell density imaging with 64Cu-labeled cys-diabody informs immunotherapy protocols. *Clin Cancer Res*. 2018;24:4976–4987.

116. Tavaré R, McCracken MN, Zettlitz KA, et al. Engineered antibody fragments for immuno-PET imaging of endogenous CD8+ T cells in vivo. *Proc Natl Acad Sci U S A*. 2014;111:1108–1113.
117. Tavaré R, Escuin-Ordinas H, Mok S, et al. An effective immuno-PET imaging method to monitor CD8-dependent responses to immunotherapy. *Cancer Res*. 2016;76:73–82.
118. Rashidian M, Ingram JR, Dougan M, et al. Predicting the response to CTLA-4 blockade by longitudinal noninvasive monitoring of CD8 T cells. *J Exp Med*. 2017;214:2243–2255.
119. Zhao H, Wang C, Yang Y, et al. ImmunoPET imaging of human CD8+ T cells with novel 68Ga-labeled nanobody companion diagnostic agents. *J Nanobiotechnology*. 2021;19:42.
120. Farwell MD, Gamache RF, Babazada H, et al. CD8-targeted PET imaging of tumor infiltrating T cells in patients with cancer: A phase I first-in-human study of ^{89} Zr-Df-IAB22M2C, a radiolabeled anti-CD8 minibody. *J Nucl Med*. 2022. https://doi.org/10.2967/jnumed.121.262485. [e-pub ahead of print]. Accessed January 22, 2022.
121. de Ruijter LK, de Donk PP van, Hooiveld-Noeken JS, et al. Abstract LB037: 89ZED88082A PET imaging to visualize CD8+ T cells in patients with cancer treated with immune checkpoint inhibitor. *Cancer Res*. 2021;81(13 Suppl). LB037-LB037.
122. Larimer BM, Wehrenberg-Klee E, Dubois F, et al. Granzyme B PET imaging as a predictive biomarker of immunotherapy response. *Cancer Res*. 2017;77:2318–2327.
123. Bhat P, Leggatt G, Waterhouse N, Frazer IH. Interferon-γ derived from cytotoxic lymphocytes directly enhances their motility and cytotoxicity. *Cell Death Dis*. 2017;8:e2836.. -e2836.
124. Topalian SL, Hodi FS, Brahmer JR, et al. Five-year survival and correlates among patients with advanced melanoma, renal cell carcinoma, or non−small cell lung cancer treated with nivolumab. *JAMA Oncol*. 2019;5:1411–1420.
125. Weber JS, Hodi FS, Wolchok JD, et al. Safety profile of nivolumab monotherapy: A pooled analysis of patients with advanced melanoma. *J Clin Oncol*. 2017;35:785–792.
126. Migden MR, Khushalani NI, Chang ALS, et al. Cemiplimab in locally advanced cutaneous squamous cell carcinoma: Results from an open-label, phase 2, single-arm trial. *Lancet Oncol*. 2020;21:294–305.
127. Barlesi F, Vansteenkiste J, Spigel D, et al. Avelumab versus docetaxel in patients with platinum-treated advanced non-small-cell lung cancer (JAVELIN Lung 200): An open-label, randomised, phase 3 study. *Lancet Oncol*. 2018;19:1468–1479.
128. Gulley JL, Rajan A, Spigel DR, et al. Avelumab for patients with previously treated metastatic or recurrent non-small cell lung cancer (JAVELIN Solid Tumor): Dose-expansion cohort of a multicentre, open-label, phase 1b trial. *Lancet Oncol*. 2017;18:599–610.
129. Garassino MC, Cho BC, Kim JH, et al. Durvalumab as third-line or later treatment for advanced non-small-cell lung cancer (ATLANTIC): An open-label, single-arm, phase 2 study. *Lancet Oncol*. 2018;19:521–536.
130. Eggermont AMM, Chiario-Sileni V, Grob JJ, et al. Prolonged survival in stage III melanoma with ipilimumab adjuvant therapy. *N Engl J Med*. 2016;375:1845–1855.
131. Wolchok JD, Chiarion-Sileni V, Gonzalez R, et al. Overall survival with combined nivolumab and ipilimumab in advanced melanoma. *N Engl J Med*. 2017;377:1345–1356.
132. Fradet Y, Bellmunt J, Vaughn DJ, et al. Randomized phase III KEYNOTE-045 trial of pembrolizumab versus paclitaxel, docetaxel, or vinflunine in recurrent advanced urothelial cancer: Results of >2 years of follow-up. *Ann Oncol*. 2019;30:970–976.
133. Gettinger S, Horn L, Jackman D, et al. Five-year follow-up of nivolumab in previously treated advanced non-small-cell lung cancer: Results from the CA209-003 study. *J Clin Oncol*. 2018;36:1675–1684.
134. Ready NE, Ott PA, Hellmann MD, et al. Nivolumab monotherapy and nivolumab plus ipilimumab in recurrent small cell lung cancer: Results from the CheckMate 032 randomized cohort. *J Thorac Oncol*. 2020;15:426–435.
135. Verhoeff S, van de Donk PP, Aarntzen EHJG, et al. 89Zr-durvalumab PD-L1 PET in recurrent or metastatic (R/M) squamous cell carcinoma of the head and neck. *J Clin Oncol*. 2020;38(15 Suppl):3573.. -3573.
136. Niemeijer ALN, Oprea Lager DE, Huisman MC, et al. First-in-human study of 89Zr-pembrolizumab PET/CT in patients with advanced stage non-small-cell lung cancer. *J Nucl Med*. 2022;63:362–367.
137. Kok IC, Hooiveld JS, van de Donk PP, et al. 89Zr-pembrolizumab imaging as a noninvasive approach to assess clinical response to PD-1 blockade in cancer. *Ann Oncol*. 2022;33:80–88.
138. Ehlerding EB, Lee HJ, Jiang D, et al. Antibody and fragment-based PET imaging of CTLA-4 + T-cells in humanized mouse models. *Am J Cancer Res*. 2019;9:53–63.
139. Pandit-Taskar N, Postow MA, Hellmann MD, et al. First-in-humans imaging with 89Zr-Df-IAB22M2C anti-CD8 minibody in patients with solid malignancies: Preliminary pharmacokinetics, biodistribution, and lesion targeting. *J Nucl Med*. 2020;61:512–519.